Organic Electronics 14 (2013) 3195–3200

Contents lists available at ScienceDirect

Organic Electronics

journal homepage: www.elsevier.com/locate/orgel

AC-driven, color- and brightness-tunable organic light-emitting diodes constructed from an electron only device

Yongbiao Zhao [a], Rui Chen [b], Yuan Gao [a,b], Kheng Swee Leck [a], Xuyong Yang [a], Shuwei Liu [a], Agus Putu Abiyasa [a], Yoga Divayana [a], Evren Mutlugun [a], Swee Tiam Tan [a], Handong Sun [b,*], Hilmi Volkan Demir [a,b,c,*], Xiao Wei Sun [a,d,*]

[a] Luminous! Center of Excellence for Semiconductor Lighting and Displays, School of Electrical and Electronic Engineering, Nanyang Technological University, 50 Nanyang Avenue, Singapore 639798, Singapore
[b] Division of Physics and Applied Physics, School of Physical and Mathematical Sciences, Nanyang Technological University, 21 Nanyang Link, Singapore 637371, Singapore
[c] Department of Physics, Department of Electrical and Electronics Engineering, and UNAM–Institute of Materials Science and Nanotechnology, Bilkent University, TR-06800 Ankara, Turkey
[d] South University of Science and Technology of China, Shenzhen, Guangdong 518055, China

ARTICLE INFO

Article history:
Received 23 July 2013
Received in revised form 12 September 2013
Accepted 14 September 2013
Available online 30 September 2013

Keywords:
Organic light-emitting diode
Alternating current
AC driving
Color tunable
Charge generation layer
Transition metal oxide

ABSTRACT

In this paper, a color- and brightness-tunable organic light-emitting diode (OLED) is reported. This OLED was realized by inserting a charge generation layer into an electron only device to form an n-i-p-i-n structure. It is shown that, by changing the polarity of applied voltage, only the p-i-n junction operated under positive bias can emit light and, by applying an AC voltage, emission from both junctions was realized. It is also shown that, by using a combination of blue- and red-emiting layers in two p-i-n junctions, both the color and brightness of the resulting white OLED can be tuned independently by changing the positive and negative amplitudes of the AC voltage.

1. Introduction

Fundamentally, light emission from an organic light-emitting diode (OLED) [1] results from the electron/hole recombination in the emissive layer (EML), which requires simultaneous hole and electron injection from the anode and the cathode, and then transport through the hole transporting layer (HTL) and the electron transporting layer (ETL), respectively, as shown in Fig. 1a. However, in a single carrier device [2], as only one charge carrier is injected into the device, light emission is impossible. For example, Fig. 1b shows an electron only device (EOD), which can be considered as an n-i-n structure. The low injection barrier for electrons and high injection barrier for holes allow only the electrons to be injected from the electrode with a negative bias across the device while the holes are blocked at the other electrode. Therefore, the electron/hole recombination is internally not possible. Single carrier devices as such were usually used to determine electrical transporting parameters [2–9], such as mobility, carrier density and trap levels. It would be very interesting if one can convert an EOD to a light-emitting device. One

* Corresponding authors. Address: Division of Physics and Applied Physics, School of Physical and Mathematical Sciences, Nanyang Technological University, 21 Nanyang Link, Singapore 637371, Singapore (H.D. Sun), Luminous! Center of Excellence for Semiconductor Lighting and Displays, School of Electrical and Electronic Engineering, Nanyang Technological University, 50 Nanyang Avenue, Singapore 639798, Singapore (H.V. Demir, X.W. Sun).

E-mail addresses: hdsun@ntu.edu.sg (H. Sun), volkan@stanfordalumni.org (H.V. Demir), exwsun@ntu.edu.sg (X.W. Sun).

1566-1199/$ - see front matter © 2013 Elsevier B.V. All rights reserved.
http://dx.doi.org/10.1016/j.orgel.2013.09.028

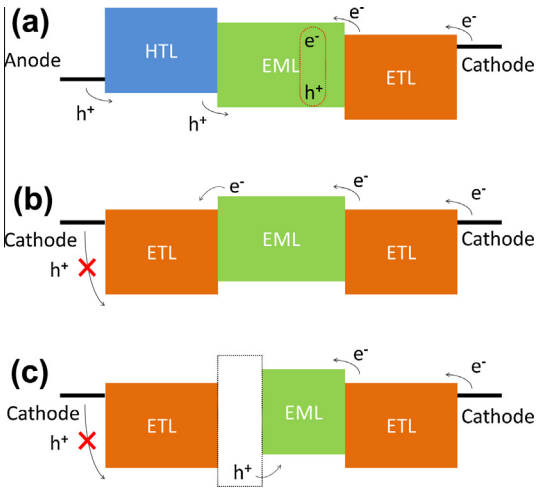

Fig. 1. Schematic energy level diagrams of a typical OLED (a), electron only device (b) and electron only device with a hole source (c).

possible way is to incorporate a hole source at one side of the EML, as shown in Fig. 1c.

Fortunately, a charge generation layer (CGL), which is generally used in tandem OLEDs [10–30], can be used to create extra charge carriers. To date, many CGL structures have been proposed, such as n-doped ETL/p-doped HTL (e.g., Alq_3:Li/NPB:$FeCl_3$) [10], organic p/n junction (e.g., Pentacene/C60) [23,24,26,27] and n-doped ETL/electron acceptor/electron donor structure (e.g., BCP:Li/MoO_3/NPB [21], Bphen:Li/HAT-CN/NPB [18]). It was previously shown that the high work function (WF) of transition metal oxides (TMOs) [31–40], such as WO_3 (WF = 6.78 eV) and MoO_3 (WF = 6.83 eV), plays an important role in the charge generation process. Many electronic structure [32–34,37,38,40] and device physics studies suggest that charge generation originates from the electron transfer from the hole transporting material to TMOs (e.g., in Bphen:Cs/MoO_3/NPB CGL, electron transfers from NPB to MoO_3), which is the core of CGL. It is thus anticipated that the incorporation of CGL in a single carrier device could enable the dual carrier injection. Qi et al. showed that a BCP:Li/MoO_3 CGL is capable of injecting both holes (device structure: Al/BCP:Li/MoO_3/NPD/MoO_3/Al) and electrons (device structure: Al/BCP/BCP:Li/MoO_3/Al) by means of charge generation [41]. Lee et al. also employed a p-doped HTL/n-doped ETL type CGL (CuPc:ReO_3/Bphen:Rb_2CO_3) as an electron injection layer in an inverted OLED structure for a p-n-i-p structure [42], which can inject electrons well and is independent of the choice of the electrode.

In this paper, we investigated the effect of a TMO (MoO_3)-based charge generation layer in an EOD and successfully converted the EOD to a light-emitting device (from n-i-n structure to n-i-p-i-n structure). Due to the symmetrical energy band diagram design, our device can be operated to emit light by both positive and negative bias. By employing a blue dye in one n-i-p junction and a red dye in another n-i-p junction, the device can emit either blue or red color, depending on the polarity of the bias. We also found that, by applying an alternating current (AC) signal, alternating blue and red emission was observed. By changing the relative positive and negative amplitudes of the AC voltage, various white colors with tunable brightness were realized, which is impossible for a conventional OLED.

2. Experimental

2.1. Device fabrication

All devices were fabricated on commercial ITO-coated glass substrates. The ITO substrates were treated in order by ultrasonic bath sonication of detergent, de-ionized water, isopropanol and acetone, each with a 20 min interval. Then the ITO substrates were dried with nitrogen gas and baked in an oven at 80 °C for 30 min. Subsequently, the substrates were transferred into a thermal evaporator, where the organic, inorganic and metal functional layers were grown layer by layer at a base pressure better than 4×10^{-4} Pa. The evaporation rates were monitored with several quartz crystal microbalances located above the crucibles and thermal boats. For organic semiconductors, metal oxides and calcium, the typical evaporation rates were about 0.1 nm/s and for aluminum, the evaporation rate was about 1–5 nm/s. For the dyes, typical evaporation rates were 0.01 nm/s, as reported in the literature [43,44]. The intersection of Al and ITO formed a 3 mm × 3 mm active device area.

2.2. Device characterization

Current density–voltage (*J*–*V*) and luminance–voltage (*L*–*V*) data were collected with a source meter (Yokogawa GS610) and a luminance meter (Konica Minolta LS-110) with a customized Labview program. Electroluminance (EL) spectra were recorded with a spectrometer (Photo Research PR705). The AC voltage used to drive the device for EL spectrum measurement was generated by the same sourcemeter (Yokogawa GS610) operating in the pulse mode (rectangular shape, 50% duty cycle, 50 Hz). For EL transient study, a function generator (Tabor Electronics

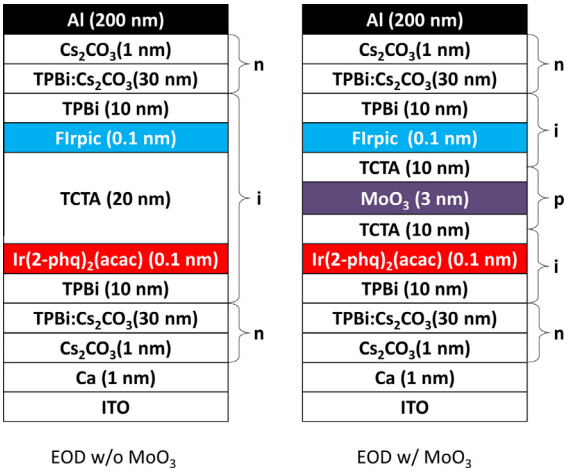

Fig. 2. Device structures for EOD w/o (left) and w/ (right) MoO_3 layer.

WW5062 50MS/s Dual-Channel Arbitrary Waveform Generator) and a high speed voltage amplifier (Tabor Electronics 9200, 300$V_{p\text{-}p}$ Dual-Channel Signal Amplifier, with a fixed gain of 50) were used to produce the AC voltage (sinusoid shape, 1 kHz), and the light was converted to an electrical signal by a photomultiplier tube (Hamamatsu R928 Photomultiplier Tube) and monitored with an oscilloscope (TEKTRONIX DPO 7254 Digital Phosphor Oscilloscope, 2.5 GHz, 400 GS/s).

3. Results and discussions

The device structures for the EOD without (w/o) and with (w/) the MoO_3 layers are shown in Fig. 2. A thin Ca/Cs_2CO_3 layer on ITO was used to lower the electron injection barrier. 1,3,5-Tri(1-phenyl-1H-benzo[d]imidazol-2-yl)phenyl (TPBi) [45] doped with 30 wt% Cs_2CO_3 was used as the ETL. Two thin films of blue and red phosphorescent dyes, bis(3,5-difluoro-2-(2-pyridyl)phenyl-(2-carboxypyrid-yl)iridium(III) (FIrpic) [46] and bis(2-phenylquinoline)(acetylacetonate)iridium(III) (Ir(2-phq)$_2$(acac)) [47], were placed at the two interfaces of TPBi and 4,4′,4″-Tri(9-carbazoyl)triphenylamine (TCTA) [48] as the blue and red EMLs, respectively. In the EOD w/o the MoO_3 layer, the two Cs_2CO_3/TPBi:Cs_2CO_3 layers can be considered as two n-regions, while the TPBi/Ir(2-phq)$_2$(acac)/TCTA/FIrpic/TPBi layers can be considered as one intrinsic region (*i*-region). Thus, the EOD w/o MoO_3

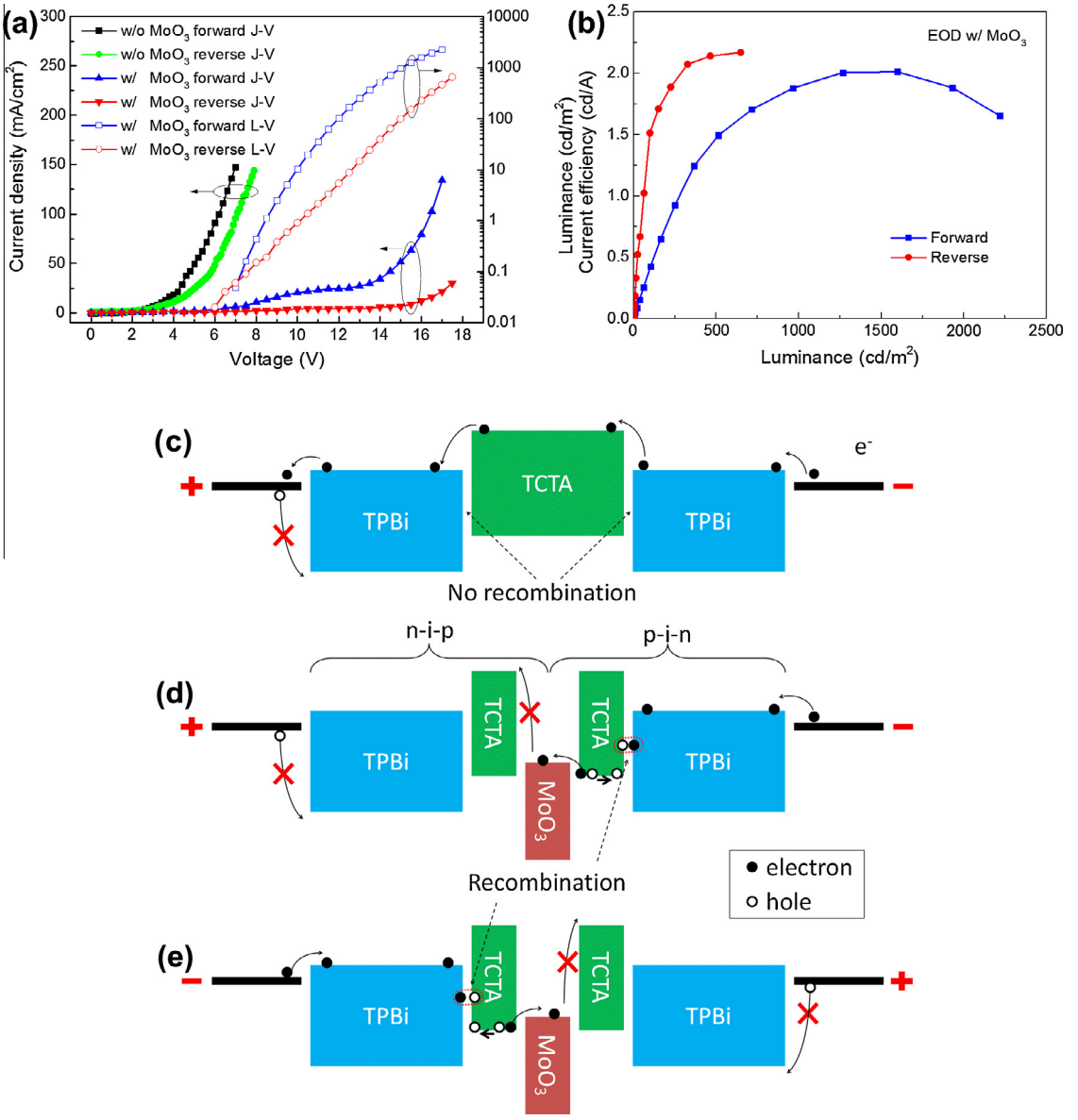

Fig. 3. (a) Current density–voltage and luminance–voltage curves of the EOD w/o and w/ MoO_3; (b) current efficiency of the EOD w/ MoO_3; schematic energy level diagrams of the EOD w/o MoO_3 under positive bias (c) and the EOD w/ MoO_3 under positive (d) and negative biases (e).

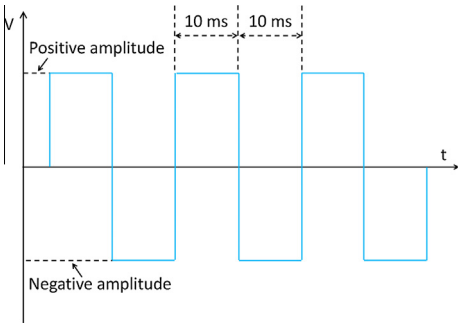

Fig. 4. Schematic view of the AC driving voltage used to drive the EOD w/ MoO_3.

has an n-i-n structure. When a thin MoO_3 layer was incorporated into the former EOD device, due to the interface hole transfer doping effect [35,49], the MoO_3 layer together with the adjacent thin TCTA layer can be considered as one p-doped region (*p*-region). Thus, the EOD w/ MoO_3 has an n-i-p-i-n structure and can be considered as two p-i-n diodes with back-to-back connection.

The *J–V* curves of the two devices are shown in Fig. 3a. Here, the forward bias implies that the ITO electrode is positively biased while Al electrode is grounded, while the reverse bias implies that the ITO electrode is negatively biased while Al electrode is grounded. For the EOD w/o MoO_3, the forward current density is a little larger than the reverse one. This agrees well with the previous literature, as in a reverse stack of Cs_2CO_3 on metal, the electron injection is not as efficient as the normal stack of metal on Cs_2CO_3 [50]. As expected, in this case, no light emission was observed in this EOD, indicating holes were blocked outside the device (as shown in Fig. 3c). When a thin MoO_3 film was introduced in the middle of TCTA layer, a significant reduction for both forward and reverse current densities is observed. This means that the introduction of MoO_3 has changed the charge carrier dynamics. As shown in Fig. 3d, when forward bias was applied, the electron and

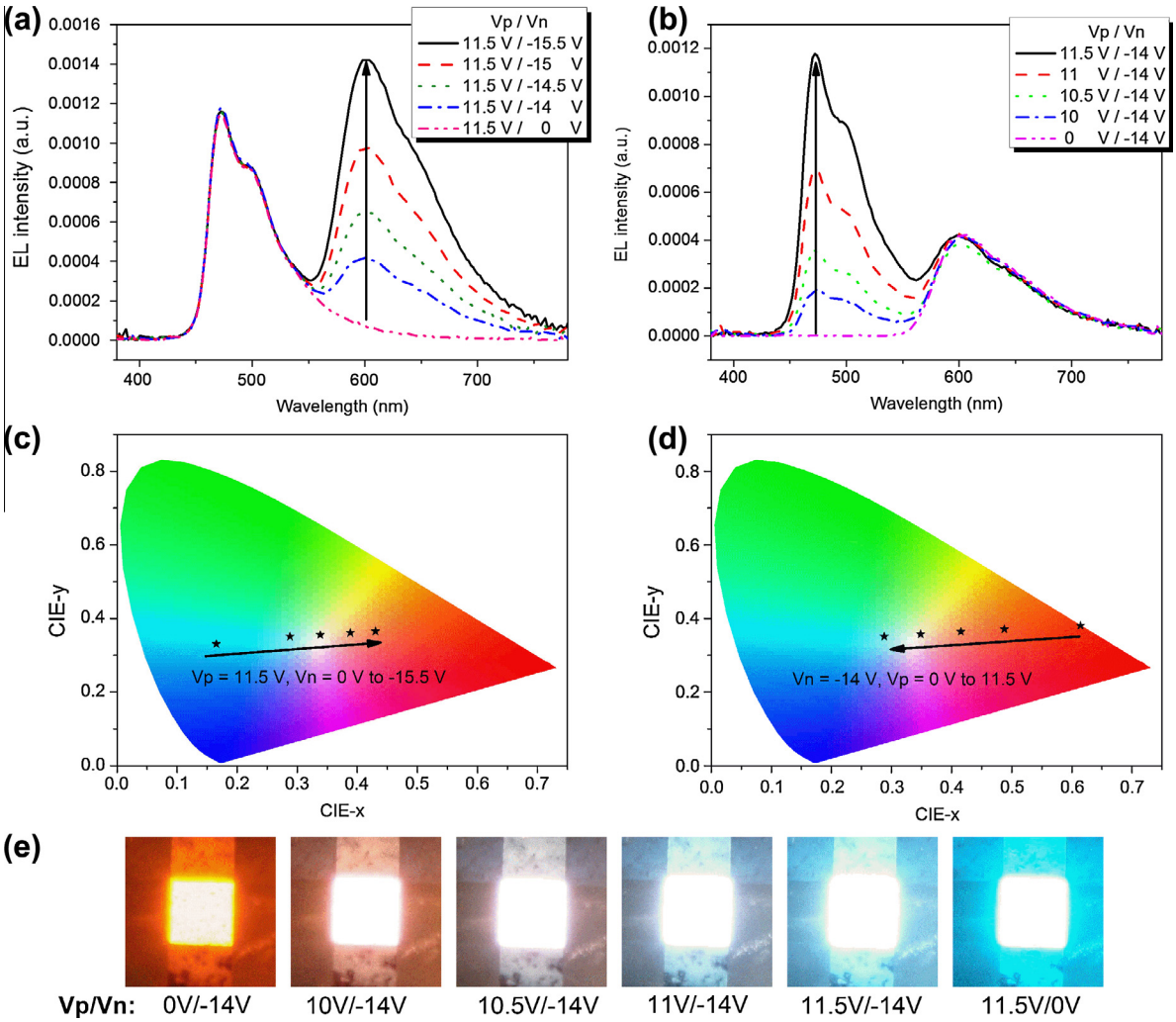

Fig. 5. EL spectra of the EOD w/ MoO_3 driven with fixed positive amplitude and variable negative amplitude AC voltages (a), and fixed negative amplitude and variable positive amplitude AC voltages (b). The corresponding variation of CIE coordinates is shown in (c) and (d). The arrows in (a)–(d) indicate the voltage increase direction. The photos of the device under different positive/negative amplitude AC voltages are shown in (e).

hole injection barriers at the electrodes were still the same as in Fig. 3c. That is, hole was blocked and electron could be injected easily. At the same time, due to the high WF of MoO_3, electrons were extracted from HOMO of TCTA to the valence band of MoO_3 while holes were left on TCTA [33]. The hole injection barrier in the p-i-n junction was thus negligible and the p-i-n junction could be easily switched on. However, for the n-i-p junction, as there was also a big electron injection barrier from MoO_3 to TCTA, both hole and electron injections in the n-i-p junction were very hard. That is, the n-i-p junction was switched off. Thus, the large reduction in the current density can be attributed to the large resistance of the n-i-p junction as a result of MoO_3 introduction. For the reverse bias condition, similar analysis applies, as shown in Fig. 3e.

From the charge carrier dynamics given in Fig. 3d and e, we can see that electron/hole recombination is possible for the p-i-n junction under positive bias. As shown in Fig. 3b, light emissions under both the positive bias and negative bias were observed. As we can see, the turn-on voltages for forward bias and reverse bias were around 6 to 7 V, respectively, about two times of traditional OLEDs. The maximum brightness in the forward bias was about 2200 cd/m^2, while in the reverse bias it was about 700 cd/m^2. The maximum current efficiencies for the forward bias and reverse bias were 2.0 and 2.1 cd/A, respectively, which correspond to external quantum efficiencies of 0.9% and 1.35%. These maximum brightness and efficiency values were much lower compared with those of conventional OLED structure, which indicates that in this device the electron/hole injection [51,52] are not balanced. It is assumed that electrons were the major charge carrier in the device, while the generated holes are much fewer in number compared with injected electrons.

From the results shown above, we know that the EOD w/ MoO_3 can be operated by both positive and negative biases. If we apply an AC voltage, we should be able to see both the blue and red emission. To demonstrate this, a rectangular AC voltage (as shown in Fig. 4) at a frequency of 50 Hz, at a duty cycle of 50% and with controllable levels of positive amplitude (V_p) and negative amplitude (V_n) was used to drive the EOD w/ MoO_3. As shown in Fig. 5a, with a fixed V_p of 11.5 V and V_n of 0 V, the device emits only blue light with a CIE 1931 color coordinates of (0.16, 0.32), which is the typical emission for FIrpic [46]. As V_n decreases to −14 V, besides the blue emission, a red emission also emerges. As V_n further decreases, the red emission grows gradually, while the blue emission intensity keeps almost unchanged. The corresponding change in CIE coordinates was shown in Fig. 5c. As we can see, as V_n decreases, the CIE coordinates move across the white zone and toward the red zone, which corresponds to a change of correlated color temperature (CCT) from 7575 to 2773 K. When V_p is 11.5 V and V_n is −14.5 V, a CIE coordinates of (0.33,0.35) was realized, which is close to the equal energy white point of (0.33, 0.33). In Fig. 5b, V_n is fixed at −14 V, when V_p is 0 V, as expected, only the red emission is observed, with a CIE coordinates of (0.61, 0.38). When V_p increases from 10 to 11.5 V gradually, the blue emission grows accordingly and the red emission keeps unchanged. In this case, the CIE coordinates move from the red zone toward the blue zone, as shown in Fig. 5d. Fig. 5e shows several photos of the EOD w/ MoO_3 at different V_p/V_n combinations. As can be seen, the device shows uniform emission with color tunablity from red to white to blue, which cannot be achieved in a conventional OLED. We should note here that, with a proper combination of V_p and V_n, the same white color can also be tuned to different brightness levels. That is, both the brightness and color of this device can be independently tuned based on this idea. We believe this property can further improve the advantages of OLEDs as the lighting sources.

To identify the EOD w/ MoO_3 indeed emits blue and red color alternatingly under AC voltage, we further studied the EL transient behavior of the device. During the experiment, the device was driven under a sinusoid AC voltage with frequency of 1 kHz, as shown in Fig. 6 (the red curve). The AC voltage amplitude was tuned to let the device emit

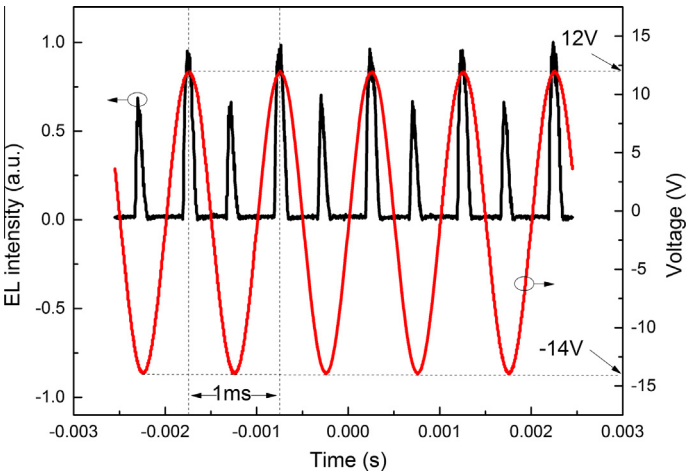

Fig. 6. Transient EL signal of the EOD w/ MoO_3 under a sinusiodal AC voltage. The amplitude of the AC voltage was 13 V and the frequency was 1 kHz and an offset of −1 V was applied. The EL signal at the positive half period corresponds to the blue emission, while the EL signal at the negative half period corresponds to the red emission. (For interpretation of the references to color in this figure legend, the reader is referred to the web version of this article.)

detectable light signal (the black curve in Fig. 6). As can be seen, there is indeed light signal at both the peaks and valleys of the AC voltage. The light signals at AC peaks (blue emission) is about two times the emission at the AC valleys (red emission), which agrees well with the L–V curves shown in Fig. 3a.

4. Conclusion

In conclusion, we demonstrated a light-emitting device, which was converted from a non-emissive electron only device. Here the key was to introduce a hole source in the device. In our case, we used a sole MoO_3 based charge generation layer. With a symmetric device structure, the new device can be operated to emit light under both positive and negative voltages. This finding indicates the important role of transition metal oxides in the charge generation layer. Furthermore, with a combination of blue and red emissive layers, the device can be used to produce white light and both the brightness and color can be tuned independently under AC voltage, which can be hardly realized in conventional OLEDs. However, the efficiency of the device is still low compared with conventional OLEDs due to unbalanced charge carrier injection, which needs further investigation.

Acknowledgements

This work is supported by the National Research Foundation of Singapore under Grant Nos. NRF-CRP-6-2010-2 and NRF-RF-2009-09, and the Singapore Agency for Science, Technology and Research (A*STAR) SERC under Grant Nos. 112 120 2009 and 092 101 0057. This work is also supported by National Natural Science Foundation of China (NSFC) (project Nos. 61006037 and 61076015).

References

[1] C.W. Tang, S.A. VanSlyke, Appl. Phys. Lett. 51 (1987) 913.
[2] P.W.M. Blom, M.J.M. deJong, J.J.M. Vleggaar, Appl. Phys. Lett. 68 (1996) 3308.
[3] P.W.M. Blom, M.J.M. deJong, M.G. vanMunster, Phys. Rev. B 55 (1997) 656.
[4] P.S. Davids, I.H. Campbell, D.L. Smith, J. Appl. Phys. 82 (1997) 6319.
[5] V.I. Arkhipov, E.V. Emelianova, Y.H. Tak, H. Bassler, J. Appl. Phys. 84 (1998) 848.
[6] P.W.M. Blom, M. Vissenberg, Phys. Rev. Lett. 80 (1998) 3819.
[7] M. Redecker, D.D.C. Bradley, M. Inbasekaran, E.P. Woo, Appl. Phys. Lett. 73 (1998) 1565.
[8] S.W. Tsang, S.K. So, J.B. Xu, J. Appl. Phys. 99 (2006) 013706.
[9] V. Coropceanu, J. Cornil, D.A. da Silva, Y. Olivier, R. Silbey, J.L. Bredas, Chem. Rev. 107 (2007) 926.
[10] L.S. Liao, K.P. Klubek, C.W. Tang, Appl. Phys. Lett. 84 (2004) 167.
[11] C.C. Chang, J.F. Chen, S.W. Hwang, C.H. Chen, Appl. Phys. Lett. 87 (2005) 253501.
[12] C.W. Chen, Y.J. Lu, C.C. Wu, E.H.E. Wu, C.W. Chu, Y. Yang, Appl. Phys. Lett. 87 (2005) 241121.
[13] F.W. Guo, D.G. Ma, Appl. Phys. Lett. 87 (2005) 173510.
[14] J.X. Sun, X.L. Zhu, H.J. Peng, M. Wong, H.S. Kwok, Appl. Phys. Lett. 87 (2005) 093504.
[15] T.Y. Cho, C.L. Lin, C.C. Wu, Appl. Phys. Lett. 88 (2006) 111106.
[16] H. Kanno, R.J. Holmes, Y. Sun, S. Kena-Cohen, S.R. Forrest, Adv. Mater. 18 (2006) 339.
[17] T.W. Lee, T. Noh, B.K. Choi, M.S. Kim, D.W. Shin, J. Kido, Appl. Phys. Lett. 92 (2008) 043301.
[18] L.S. Liao, K.P. Klubek, Appl. Phys. Lett. 92 (2008) 223311.
[19] Q.Y. Bao, J.P. Yang, J.X. Tang, Y.Q. Li, C.S. Lee, S.T. Lee, Org. Electron. 11 (2010) 1578.
[20] S. Hamwi, J. Meyer, M. Kroger, T. Winkler, M. Witte, T. Riedl, A. Kahn, W. Kowalsky, Adv. Func. Mater. 20 (2010) 1762.
[21] X. Qi, N. Li, S.R. Forrest, J. Appl. Phys. 107 (2010) 014514.
[22] K.S. Yook, S.O. Jeon, S.Y. Min, J.Y. Lee, H.J. Yang, T. Noh, S.K. Kang, T.W. Lee, Adv. Func. Mater. 20 (2010) 1797.
[23] Y.H. Chen, J.S. Chen, D.G. Ma, D.H. Yan, L.X. Wang, J. Appl. Phys. 110 (2011) 074504.
[24] Y.H. Chen, J.S. Chen, D.G. Ma, D.H. Yan, L.X. Wang, F.R. Zhu, Appl. Phys. Lett. 98 (2011) 243309.
[25] Y.M. Cheng, H.H. Lu, T.H. Jen, S.A. Chen, J. Phys. Chem. C 115 (2011) 582.
[26] Y.H. Chen, D.G. Ma, J. Mater. Chem. 22 (2012) 18718.
[27] Y.H. Chen, H.K. Tian, J.S. Chen, Y.H. Geng, D.H. Yan, L.X. Wang, D.G. Ma, J. Mater. Chem. 22 (2012) 8492.
[28] B.F. Ding, X.Y. Hou, K. Alameh, Appl. Phys. Lett. 101 (2012) 133305.
[29] J. Meyer, S. Hamwi, M. Kroger, W. Kowalsky, T. Riedl, A. Kahn, Adv. Mater. 24 (2012) 5408.
[30] J.P. Yang, Q.Y. Bao, Y. Xiao, Y.H. Deng, Y.Q. Li, S.T. Lee, J.X. Tang, Org. Electron. 13 (2012) 2243.
[31] X.D. Gao, J. Zhou, Z.T. Xie, B.F. Ding, Y.C. Qian, X.M. Ding, X.Y. Hou, Appl. Phys. Lett. 93 (2008) 083304.
[32] D.Y. Kim, J. Subbiah, G. Sarasqueta, F. So, H.J. Ding, Irfan, Y.L. Gao, Appl. Phys. Lett. 95 (2009) 093304.
[33] M. Kroeger, S. Hamwi, J. Meyer, T. Riedl, W. Kowalsky, A. Kahn, Appl. Phys. Lett. 95 (2009) 123301.
[34] M. Kroger, S. Hamwi, J. Meyer, T. Riedl, W. Kowalsky, A. Kahn, Org. Electron. 10 (2009) 932.
[35] Z.Y. Chen, I. Santoso, R. Wang, L.F. Xie, H.Y. Mao, H. Huang, Y.Z. Wang, X.Y. Gao, Z.K. Chen, D.G. Ma, A.T.S. Wee, W. Chen, Appl. Phys. Lett. 96 (2010) 213104.
[36] K. Kanai, K. Koizumi, S. Ouchi, Y. Tsukamoto, K. Sakanoue, Y. Ouchi, K. Seki, Org. Electron. 11 (2010) 188.
[37] J. Meyer, K. Zilberberg, T. Riedl, A. Kahn, J. Appl. Phys. 110 (2011) 033710.
[38] M.T. Greiner, M.G. Helander, W.M. Tang, Z.B. Wang, J. Qiu, Z.H. Lu, Nat. Mater. 11 (2012) 76.
[39] Y.B. Zhao, J.S. Chen, W. Chen, D.G. Ma, J. Appl. Phys. 111 (2012) 043716.
[40] J.Q. Zhong, H.Y. Mao, R. Wang, J.D. Lin, Y.B. Zhao, J.L. Zhang, D.G. Ma, W. Chen, Org. Electron. 13 (2012) 2793.
[41] X. Qi, N. Li, S.R. Forrest, J. Appl. Phys. 107 (2010) 8.
[42] J.H. Lee, J.W. Kim, S.Y. Kim, S.J. Yoo, J.J. Kim, Org. Electron. 13 (2012) 545.
[43] Y.B. Zhao, J.S. Chen, D.G. Ma, Appl. Phys. Lett. 99 (2011) 163303.
[44] Y.B. Zhao, J.S. Chen, D.G. Ma, ACS Appl. Mater. Interf. 5 (2013) 965.
[45] Z.Q. Gao, C.S. Lee, I. Bello, S.T. Lee, R.M. Chen, T.Y. Luh, J. Shi, C.W. Tang, Appl. Phys. Lett. 74 (1999) 865.
[46] R.J. Holmes, S.R. Forrest, Y.J. Tung, R.C. Kwong, J.J. Brown, S. Garon, M.E. Thompson, Appl. Phys. Lett. 82 (2003) 2422.
[47] S. Lamansky, P. Djurovich, D. Murphy, F. Abdel-Razzaq, R. Kwong, I. Tsyba, M. Bortz, B. Mui, R. Bau, M.E. Thompson, Inorg. Chem. 40 (2001) 1704.
[48] Y. Kuwabara, H. Ogawa, H. Inada, N. Noma, Y. Shirota, Adv. Mater. 6 (1994) 677.
[49] W. Chen, S. Chen, D.C. Qi, X.Y. Gao, A.T.S. Wee, J. Am. Chem. Soc. 129 (2007) 10418.
[50] E. Najafabadi, K.A. Knauer, W. Haske, C. Fuentes-Hernandez, B. Kippelen, Appl. Phys. Lett. 101 (2012) 023304.
[51] L.S. Hung, C.W. Tang, M.G. Mason, Appl. Phys. Lett. 70 (1997) 152.
[52] J.E. Malinsky, G.E. Jabbour, S.E. Shaheen, J.D. Anderson, A.G. Richter, T.J. Marks, N.R. Armstrong, B. Kippelen, P. Dutta, N. Peyghambarian, Adv. Mater. 1 (1999) 231.